Reverse-selective diffusion in nanocomposite membranes

Reghan J. Hill*
Department of Chemical Engineering and McGill Institute for Advanced Materials, McGill University
Montreal, Quebec, CANADA H3A 2B2
(Dated: March 23, 2022)

The permeability of certain polymer membranes with impenetrable nanoinclusions increases with the particle volume fraction (Merkel, *et al.*, *Science*, 296, 2002). This intriguing observation contradicts even qualitative expectations based on Maxwell's classical theory of conduction/diffusion in composites with homogeneous phases. This letter presents a simple theoretical interpretation based on classical models of diffusion and polymer physics. An essential feature of the theory is a polymer-segment depletion layer at the inclusion-polymer interface. The accompanying increase in free volume leads to a significant increase in the local penetrant diffusivity, which, in turn, increases the bulk permeability while exhibiting reverse selectivity. This model captures the observed dependence of the bulk permeability on the inclusion size and volume fraction, providing a straightforward connection between membrane microstructure and performance.

Polymer membranes facilitate a variety of molecular separations. Because their micro-structural scale is comparable to the size of solute molecules, the polymer architecture can be tailored to separate specific gas mixtures. Merkel *et al.* [8] recently showed that incorporating nanometer sized inorganic particulates into certain amorphous polymer melts increased the membrane permeability and selectivity. Because of its significant technological applications, this discovery has stimulated many experimental investigations [4, 9, 11, 12]. A theory that quantifies how the inclusion size and concentration affect the permeability and selectivity does not exist. Indeed, Merkel *et al.* highlighted that classical Maxwell-like theories fail to describe even the qualitative trends.

This letter presents a theoretical interpretation based on classical models of diffusive transport and polymer physics. Despite its simplicity, the model accurately describes experimental trends. The principal assumption is that there exists a repulsive interaction between the nanoinclusions and polymer segments. This hypothesis is support, in part, by transmission electron microscopy (TEM) images of silica-based nanocomposites [*e.g.*, 1, 8], which show clear evidence of particle aggregation.

For steady gas permeation across a membrane with thickness L, the diffusive flux is

$$|\langle \boldsymbol{j} \rangle| = -D^e \Delta n / L, \tag{1}$$

where D^e is the effective diffusivity and Δn is the differential concentration of the diffusing solute. Because the solute concentrations at the gas-membrane interfaces are proportional to the partial pressure p, with a constant of proportionality H (Henry's constant), it is customary to express the flux in terms of the differential partial pressure Δp:

$$|\langle \boldsymbol{j} \rangle| = -D^e H \Delta p. \tag{2}$$

The permeability is defined as $|\langle \boldsymbol{j} \rangle|/|\Delta p| = D^e H$. In this work, the gas solubility is assumed to be independent of solids concentration, so the inclusions influence the permeability only through their role in modifying the effective diffusivity D^e.

If voids in the polymer are much larger than the solute molecules, then the diffusivity in these voids D will be much larger than in the polymer D^∞. When $D/D^\infty \to \infty$, Maxwell's theory yields an effective diffusivity $D^e = D^\infty(1 + 3\phi_v) + O(\phi_v^2)$, where ϕ_v is the (small) volume fraction of (spherical) voids. Under these conditions, the relative enhancement of all effective diffusivities are the same, so membrane selectivity is unaltered.

Merkel *et al.*'s experiments exhibit *reverse selectivity*, meaning that the permeability of larger molecules is enhanced more than smaller ones. This necessitates molecular-scale perturbations to the polymer microstructure, precluding the notion that the permeability is enhanced by a shell of void space between the (impenetrable) inclusions and surrounding polymer. Rather, it suggests a continuous increase in the free volume when approaching the solid-polymer interface. Figure 1 depicts a single impenetrable sphere embedded in a polymer melt where polymer segments are repelled from the solid surface. This is the microstructural view that underlies the theory presented below.

Cohen and Turnbull's statistical mechanical theory [2] yields a solute diffusion coefficient

$$D = A \exp\left(-\gamma v_m / v_f\right) \tag{3}$$

where A and γ are constants, v_m is the minimum free volume required for a solute molecule to escape its cage of neighboring atoms and, hence, undergo diffusive migration, and v_f is the available free volume per volume occupying element. In this work, the volume occupying elements are the atoms of the polymer melt. For simplicity, each atom is assumed to occupy, on average, a volume v_0, where $v_0^{1/3}$ is of the order of a covalent bond length (≈ 1.5 Å). By considering the total volume, which comprises the sum of free and occupied volume, it follows

*Electronic address: reghan.hill@mcgill.ca

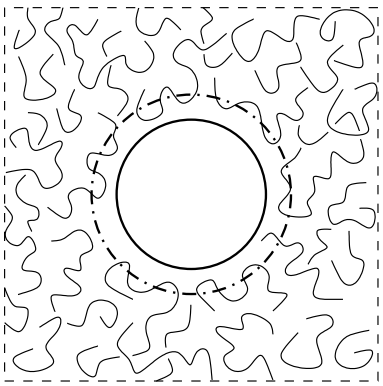

FIG. 1: An impenetrable nanosphere with radius $a \sim 5$ nm embedded in a polymer matrix with correlation length $\xi \sim 1$ nm. A repulsive interaction between the inclusion and the polymer produces a surface layer (with thickness $\sim \xi$) where the polymer segment density approaches zero. The local increase in free volume v_f (within the *dash-dotted* circle) increases the penetrant diffusivity, leading to a significant increase in the bulk permeability when $\xi \geq a$ (see figure 2).

that

$$v_f = v_0[m_1/(v_0 n_1 \rho) - 1], \tag{4}$$

where c_0 is the average atomic concentration, m_1 is the mass of a monomer (repeat unit), n_1 is the number of atoms per monomer, and ρ is the (mass) density.

A tractable analytical expression for the radial polymer segment density is obtained from a self-consistent mean-field model, with the so-called ground-state approximation and a flat interface [3]. The influence of curvature (finite inclusion radius) is of secondary importance, and is therefore neglected here. With a repulsive interaction between the polymer segments and the solid, the segment concentration is [3]

$$c(r) = c_\infty \tanh^2[(r-a)/\xi] + O(\xi/a) \tag{5}$$

where c_∞ is the bulk concentration, and $\xi = l/\sqrt{3vc_\infty}$ is the polymer correlation length, with l the segment length and v the excluded volume (per segment). Conservation of chain contour length and mass requires

$$\phi = cl^3 = (\rho/m_1)l_1 l^2, \tag{6}$$

where l_1 is the length of a monomer. Combining Eqns. (3)–(6) gives

$$D = D^\infty \exp\left[-\frac{v_m^* \phi^*(\phi - \phi_\infty)}{(1-\phi^*\phi)(1-\phi^*\phi_\infty)}\right], \tag{7}$$

where $\phi^* = n_1 v_0/(l_1 l^2)$ and $v_m^* = \gamma v_m/v_0$ are dimensionless parameters that reflect the prevailing atomic and molecular geometry.

Let us simplify matters by assuming that the bulk polymer concentration $\phi_\infty = c_\infty l^3 \approx 1$ and $v \approx l^3$, so $l^2 \approx m_1/(l_1\rho)$, $\xi \approx l/\sqrt{3}$, and $\phi^* \approx n_1 v_0 \rho/m_1$. Under these conditions, $1-\phi^*$ is the fractional free volume of the bulk polymer, and the (maximum) diffusivity at the solid-polymer interface becomes

$$D(r=a) \approx D^\infty \exp\left[v_m^* \phi^*/(1-\phi^*)\right]. \tag{8}$$

Clearly, the diffusivity at the interface can be much larger than in the bulk when $\phi^* < 1$ and $v_m^* < 10$. Note that reverse selectivity prevails, because the diffusivity decreases continuously with increasing radial distance from the solid-polymer interface.

Consider, for example, bulk poly(p-trimethylsilyl styrene) (PTMSS), for which $n_1 = 28$, $m_1 = 180.3$ g/mol, $l_1 \approx 3$ Å (two C-C bonds) and $\rho \approx 965$ kg/m^3 [7]. With $\phi_\infty = 1$, $l \approx 1.02$ nm, $\xi \approx 0.59$ nm and $\phi^* = 0.090 v_0$ (with $v_0^{1/3}$ measured in Å). To determine an appropriate value for v_0, which, in principle, should not vary significantly from one polymer to another, let us adopt a reported value of the fractional free volume $1-\phi^* = 0.191$ [7]. This provides $v_0^{1/3} \approx 2.0$ Å and $v_f^{1/3} \approx 1.3$ Å, which are both of the expected magnitude.

With a statistically homogeneous microstructure, the average diffusive flux can be expressed as a volume average

$$\langle \boldsymbol{j} \rangle = V^{-1} \int_V \boldsymbol{j} \mathrm{d}V, \tag{9}$$

where the integration extends over the discrete and continuous phases of a representative elementary volume V. The local diffusive flux is $\boldsymbol{j} = -D\boldsymbol{\nabla} n$ (Fick's first law) where n is the solute concentration. Under steady conditions, conservation demands

$$\boldsymbol{\nabla} \cdot (D\boldsymbol{\nabla} n) = 0, \tag{10}$$

where $D(r)$ is given by Eqns. (5) and (7). When the volume fraction $\phi_p = n_p(4/3)\pi a^3 \ll 1$, the average flux is [5]

$$\langle \boldsymbol{j} \rangle \approx -D^\infty \langle \boldsymbol{\nabla} n \rangle + 3\phi_p (B/a^3) D^\infty \langle \boldsymbol{\nabla} n \rangle + O(\phi_p^2), \tag{11}$$

where $\langle \boldsymbol{\nabla} n \rangle = H\Delta p/L$ is the average concentration gradient and B is the dipole strength, *i.e.*,

$$n \to \langle \boldsymbol{\nabla} n \rangle \cdot \boldsymbol{r} + B\langle \boldsymbol{\nabla} n \rangle \cdot \boldsymbol{r} r^{-3} \text{ as } r \to \infty. \tag{12}$$

In this work, B is obtained from an efficient numerical solution of Eqn. (10) that satisfies Eqn. (12) as $r \to \infty$ with a no-flux boundary condition at $r = a$[13].

The results are calculated with $\phi_\infty = 1$ and $\phi^* = 0.8$. The two remaining independent (dimensionless) parameters are the scaled correlation length ξ/a and the scaled tracer size $v_c^* = \gamma v_m/v_0$. Here, the principal influence of v_m^* is to set the diffusion coefficient at the interface: $D(r=a)/D^\infty = \exp(4v_m^*)$.

As expected, all values of $v_m^* > 0$ increase the effective diffusivity, because the available free volume increases with respect to the unperturbed (bulk) polymer. Also,

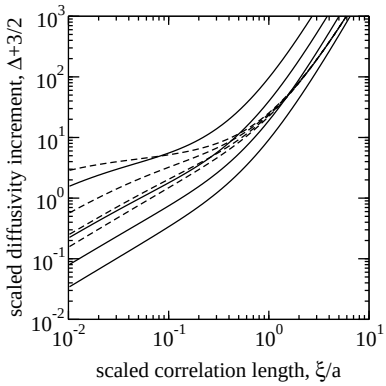

FIG. 2: The scaled diffusivity increment $\Delta = (D^e/D^\infty - 1)/\phi_p$ versus the scaled polymer correlation length ξ/a with $v_m^* = \gamma v_m/v_0 = 0.1$, 0.2, 0.4 and 1.0 (increasing upward), and $\phi^* = 0.8$ (*solid lines*). The *dashed lines* are exact solutions (Eqn. 14) for impenetrable inclusions with a uniform coating of thickness ξ where $D(a < r < a + \xi)/D^\infty = \exp(4v_m^*)$.

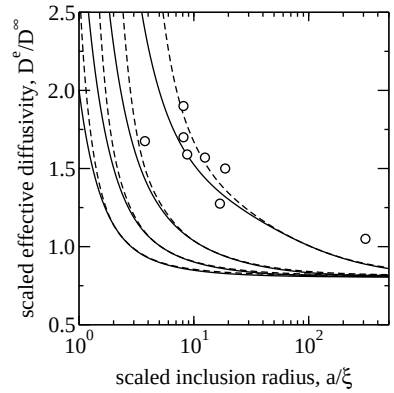

FIG. 3: The scaled effective diffusivity D^e/D^∞ versus the scaled inclusion radius a/ξ with $v_m^* = \gamma v_m/v_0 = 0.1$, 0.2, 0.4 and 1.0 (increasing upward), $\phi^* = 0.8$, and $\phi_p = 0.13$: $O(\phi_p)$ (solid lines); $O(\phi_p^2)$ (dashed lines). The *circles* are experimental measurements of the permeability enhancement from [8] (reported radii scaled with $\xi = 0.8$ nm).

because the relative increase in diffusivity depends exponentially on the penetrant size (Eqn. (8)), situations with multiple diffusing species exhibit reverse selectivity [8].

Figure 2 presents the most general predictions of the theory. The diffusivity increment, defined as

$$\Delta = -3B/a^3 = (D^e/D^\infty - 1)/\phi_p + O(\phi_p), \qquad (13)$$

is plotted as a function of the scaled correlation length ξ/a for various values of v_m^* (*solid lines*). These calculations are compared with the exact solution for an impenetrable sphere with a uniform coating (*dashed lines*):

$$\Delta = -3(1+\xi/a)^3 \frac{(1-\beta)[1+\alpha(1+\xi/a)^3]+3\beta}{(2+\beta)[1+\alpha(1+\xi/a)^3]-3\beta}. \qquad (14)$$

Here, $\beta = D/D^\infty$, with D the diffusivity inside the coating ($a < r < a + \xi$), ξ is the coating thickness, and $\alpha = 2$ [14]. The figure demonstrates that the effective diffusivity from Eqn. (3) is much more sensitive to the layer characteristics, particularly when the layers are thick ($\xi/a > 1$).

To compare the theory with the available experimental data, figures 3 and 4 show the relative effective diffusivity D^e/D^∞ and measured values of the relative permeability $D^eH/(D^\infty H^\infty)$ (*circles*), with $\phi_p = 0.13$. The $O(\phi_p)$ theory (*solid lines*) neglects particle interactions, so the values are as given by Eqn. (11). The *dashed lines* are an $O(\phi^2)$ theory, which has elements of a self-consistent mean-field approximation with an explicit correction for interactions between pairs of particles in a statistically homogeneous dispersion [6]. Note that the (single particle) dipole strength and particle concentration both affect two-body interactions.

Some of the experimental scatter in figure 3 may be attributed to the variety of filler particles (all embedded in poly(4-methyl-2-pentyne) (PMP)) and, possibly, different penetrant species and degrees of particle aggregation [8]. Nevertheless, with the foregoing approximations, the correlation length inferred by the fit is $\xi = 0.8$ nm (with $\phi^* = 0.8$) and, hence, the segment length $l \approx \sqrt{3}\xi \approx 1.4$ nm. The repeating unit of PMP comprises two C-C bonds, so there are about 4.5 monomer units per statistical segment, which is reasonable because polymers with much less "bulky" side groups (*e.g.*, poly(oxyethylene)) have fewer than two repeat units per statistical segment [*e.g.* 10, pg. 168].

Figure 4 shows how the effective diffusivity (with $a = 6.5$ nm) increases with the solid volume fraction. The theory is presented with a correlation length $\xi = 0.8$ nm, which follows from the data in figure 3, so $\xi/a = 0.8/6.5 \approx 0.123$. Despite the experimental data extrapolating to a value of $D^e < D^\infty$ as $\phi_p \to 0$, the theoretical and experimental trends are in good agreement. For reference, the *dash-dotted* line is Maxwell's self-consistent theory for impenetrable inclusions in an unperturbed polymer matrix. It is remarkable, perhaps, that a perturbation extending only $\xi \approx 0.8$ nm from the inclusion surfaces can have such a significant influence on the bulk permeability.

Theoretical predictions of the effective diffusivity have been compared with experimental measurements of the

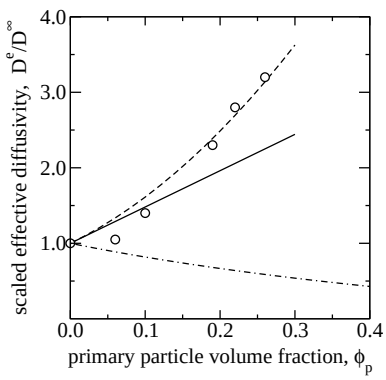

FIG. 4: The scaled effective diffusivity D^e/D^∞ versus the inclusion volume fraction ϕ_p with $v_m^* = \gamma v_m/v_0 = 1.0$, $\phi^* = 0.8$ and $\xi/a = 0.8/6.5 \approx 0.123$: exact $O(\phi_p)$ theory (*solid lines*); approximate $O(\phi_p^2)$ theory (*dashed lines*). The *circles* are experimental measurements of the permeability enhancement from [8] (with $a = 6.5$ nm). The *dash-dotted line* is Maxwell's self-consistent theory for impenetrable inclusions and unperturbed (homogeneous) polymer.

relative permeability. Therefore, the solubility was assumed independent of the inclusion concentration. Further, a mean-field description of the polymer segment density was adopted, with a flat, repulsive interface where the segment concentration vanishes (at $r = a$). Also, the diffusion coefficient was assumed to follow Cohen and Turnbull's formula (Eqn. (3)), with the occupied volume assumed proportional to the atomic number density. Finally, theoretical predictions were based on a statistically homogeneous dispersion of inclusions, whereas the particles are often found to aggregate. Nevertheless, the semi-quantitative agreement of theory and experiment strongly suggests that reverse selectivity in these nanocomposite membranes is of classical origin.

Acknowledgments

Supported by the Natural Sciences and Engineering Research Council of Canada (NSERC), through grant number 204542, and the Canada Research Chairs program (Tier II). The author is grateful to M. Maric (McGill University) for helpful discussions related to this work.

[1] A. Bansal, H. Yang, C. Li, K. Cho, B. C. Benicewicz, S. K. Kumar, and L. S. Schadler. Quantitative equivalence between polymer nanocomposites and thin polymer films. *Nature Materials*, 4, 2005.

[2] M. H. Cohen and D. Turnbull. Molecular transport in liquids and glasses. *J. Chem. Phys.*, 31:1164–1169, 1959.

[3] P. G. de Gennes. *Scaling Concepts in Polymer Physics*. Cornell University Press, 1979.

[4] D. Gomes, S. P. Nunes, and J.-V. Peinemann. Membranes for gas separation based on poly(1-trimethylsilyl-1-propyne)-silica nanocomposites. *J. Membr. Sci.*, 246:13–25, 2005.

[5] R. J. Hill. Transport in polymer-gel composites: Theoretical methodology and response to an electric field. *J. Fluid Mech. (In press)*, 2005.

[6] D. J. Jeffrey. Conduction through a random suspension of spheres. *Proc. R. Soc. Lon. A*, 335(1602):355–367, 1973.

[7] V. S. Khotimskii, V. G. Filippova, I. S. Bryantseva, V. I. Bondar, V. P. Shantarovich, and Y. P. Yampolskii. Synthesis, transport, and sorption properties and free volume of polystyrene derivatives containing Si and F. *J. Appl. Poly. Sci.*, 78:1612–1620, 2000.

[8] T. C. Merkel, B. D. Freeman, R. J. Spontak, Z. He, I. Pinnau, P. Meakin, and A. J. Jill. Ultrapermeable, reverse-selective nanocomposite membranes. *Science*, 296:519–522, 2002.

[9] T. C. Merkel, L. G. Toy, A. L. Andrady, H. Gracz, and E. O. Stejskal. Investigation of enhnaced free volume in nanosilica-filled poly(1-trimethylsilyl-1-propyne) by ^{129}Xe NMR spectroscopy. *Macromolecules*, 36:353–358, 2003.

[10] W. B. Russel, D. A. Saville, and W. R. Schowalter. *Colloidal Dispersions*. Cambridge University Press, 1989. Paperback edition 1991.

[11] P. Winberg, K. DeSitter, C. Dotremont, S. Mullens, I. F. J. Vankelecom, and F. H. J. Maurer. Free volume and interstitial mesopores in silica filled poly(1-trimethlysilyl-1-propyne) nanocomposites. *Macromolecules*, 38:3776–3782, 2005.

[12] J. Zhong, G. Lin, W.-Y. Wen, A. A. Jones, S. Kelman, and B. D. Freeman. Translation and rotation of penetrants in ultrapermeable nanocomposite membrane of poly(2,2-bis(trifluoromethyl)-4,5-difluoro-1,3-dixole-*co*-tetrafluoroethylene) and fumed silica. *Macromolecules*, 38:3754–3764, 2005.

[13] For impenetrable inclusions (*e.g.*, non-porous silica), $D = 0$ when $r < a$.

[14] With $\alpha = (2 + D_0/D)/(1 - D_0/D)$, Eqn. (14) provides a solution for penetrable inclusions, where D_0 is the diffusivity when $r < a$ and, again, D is the diffusivity when $a < r < a + \xi$.